

Experimental Section

Synthetic Procedures and Characterization of 1-3.

Ultrapure anhydrous $\text{Ce}^{\text{III}}\text{Cl}_3$ and $\text{Ti}(\text{OEt})_4$ were acquired from Acros and Alfa-Aesar chemical companies. EtOH were acquired from Sigma-Aldrich and further dried by distillation over Mg. All analytical and spectroscopic samples were prepared inside a Saffron Scientific (type β) glovebox, equipped with a closed loop recirculation system for the removal of moisture and oxygen (operating at ca. 2.1-2.5 vppm O_2). IR spectra were recorded using a *PerkinElmer* Spectrum 100 with *Universal ATR*. X-ray diffraction (XRD) experiments were performed using an X'Pert Data Collector (PANalytical BV, The Netherlands) with $\text{Cu K}\alpha$ ($\lambda=0.1540598\text{\AA}$) radiation and the scanning angle ranged from 10° to 70° of 2θ . Both carbon and hydrogen analyses were done using a Perkin-Elmer 240 Elemental analyzer. NMR samples were dissolved in 0.75ml of dry, CD_2Cl_2 in the glovebox in Wilmad 528PP NMR tubes and were sealed with tight-fitting caps and Parafilm© prior to immediate acquisition of the spectra. Standard (1D) ^1H and ^{13}C NMR and 2D ^1H - ^1H correlation spectroscopy (COSY) spectra were recorded using a Bruker Advance Cryo Ultrashield 500 MHz spectrometer (500.05 MHz for ^1H , 125.7 MHz for ^{13}C), with both being referenced to the solvent peaks. UV-visible spectra of powdered samples of **A**, **B** and **C** were recorded in diffuse reflectance mode using a Perkin Elmer Lambda 12 UV-visible spectrometer equipped with an integration sphere (Labsphere RSA-PE-20) and referenced to a white PTFE standard (spectra shown in Figure 3).

Synthesis and Characterisation of 2 and 3

$\text{Ti}(\text{OEt})_4$ (3.5 ml, 15.4 mmol), CeCl_3 (0.246g, 1mmol) and EtOH (7ml) was placed in an autoclave under nitrogen and the mixture heated to 160°C for 3 days. Light yellow crystals of **1** were obtained directly from the reaction mixture by slow cooling to room temperature (1°C/h). Orange crystals of **2** and yellow crystals of **3** were obtained by cooling the solution obtained to room temperature (0.20g; 9 % with respect to CeCl_3 supplied).⁸ Storage of the filtrate at room temperature (ca, 3d) lead to gradual deposition of light yellow crystals of **3** (0.20g, 12.3 % with respect to CeCl_3 supplied). Further storage gave at room temperature (7d) gave large orange crystals of **2** (0.10g, 7.2 % with respect to CeCl_3 supplied).

For **2**: Elemental analysis (%) calcd. C 32.5, H 6.9; found C 30.8, H 6.0. IR ($650\text{-}4000\text{cm}^{-1}$, Nujol), ν/cm^{-1} = 690(m), 772(s), 891(m), 905(m), 914(m), 1045(vs), 1099(s), 1139(s), 1353(w), 1372(m), 1440(w), 1469(w), 2698(w), 2732(w), 2851(m), 2873(m), 2922(m), 2970(m), 3331(w) (O-H str.). ^1H NMR (500.1 MHz, $+25^\circ\text{C}$, $\text{C}_2\text{D}_2\text{Cl}_2$, δ ppm), indicated paramagnetic character as expected for $4f^1$ configuration of Ce^{3+} , collection of multiplets in the ranges 5.1-4.0 ($\text{CH}_2\text{-O}$) and 1.8-0.9 (CH_3). ^{13}C NMR ($+25^\circ\text{C}$, $\text{C}_2\text{D}_2\text{Cl}_2$, δ ppm): 72.9-67.2 (collections of singlets, OCH_2CH_3) and 30.9-17.9 (collection of singlets $-\text{OCH}_2\text{CH}_3$).

For **3**: Elemental analysis (%) calcd. C 31.2, H 6.7; found C 30.0, H 6.4. IR ($650\text{-}4000\text{ cm}^{-1}$), ν/cm^{-1} = 788(w), 850(w), 891(m), 912(m), 1043(vs), 1063(s), 1094(s), 1120(s), 1353(w), 1374(m), 1440(w), 1469(w), 2704(w), 2740(w), 2859(m), 2924(m), 2968(m), 3321(w) (O-H str.). ^1H NMR (500.1 MHz, $+25^\circ\text{C}$, $\text{C}_2\text{D}_2\text{Cl}_2$, δ ppm), indicated paramagnetic character as expected for $4f^1$ configuration of Ce^{3+} ,

collection of overlapping multiplets in the ranges 5.1-4.2 (CH₂-O) and 1.8-0.8 (CH₃). ¹³C NMR (+25°C, C₂D₂Cl₂, δ ppm): 72.9-68.2 (-OCH₂CH₃) and 30.9-17.9 (-OCH₂CH₃).

Preparation of A, B and C

0.4g crystals of cage **1** was dissolved in 60ml 50% ethanol aqueous solution and then stirred under ultrasound. After filtering the suspension and drying under 150 °C,(16h) a light yellow powder of **A** was obtained.

0.4g crystals of cage **2** was dissolved in 60ml 50% ethanol aqueous solution and then stirred under ultrasound. After filtering the suspension and drying under 150 °C (16h), a yellow powder of **B** was obtained.

0.4g crystals of cage **3** was dissolved in 60ml 50% ethanol aqueous solution and then stirred under ultrasound. After filtering the suspension and drying under 150 °C (16h), a dark yellow powder of **C** was obtained.

Elemental Analysis of **A**, **B** and **C**

A, C 0.0, H 0.6%; **B**, C 0.6, H 1.5%; **C** 0.7% C, C 0.7, H 1.2%.

These results can be compared to XPS and EDS measurements which give far higher C content, presumably because they overestimate the C content at which is at the surface of the samples.

Single-Crystal X-ray Crystallography

Crystals were mounted on glass fibers with oil. Data were collected on a Nonius KappaCCD diffractometer. The structures were solved by Direct Methods and refined by full-matrix least squares on F^2 . (SHELX, Sheldrick, G. M. *Acta Crystallogr.* **2008**, *A64*, 112).

Table SI-1 Details of the structure solutions and refinements of **2** and **3**.

Compound	2 (CCDC 923499)	3 (CCDC 923500)
Chemical formula	C ₄₄ H ₁₁₁ CeO ₂₉ Ti ₈ CeTi ₈ O ₇ (HOEt)(OEt) ₂₁	C ₃₆ H ₉₂ Cl ₂ Ce ₂ O ₂₀ Ti ₄ [{Ti ₂ O(OEt) ₈ }(EtOH·CeCl)] ₂
FW	1627.65	1387.84
Crystal system	Monoclinic	Monoclinic
Space group	<i>C</i> 2/ <i>c</i>	<i>P</i> 21/ <i>n</i>
Unit cell dimensions		
<i>a</i> (Å)	15.630(4)	11.9651(6)
<i>b</i> (Å)	23.318(5)	19.4670(12)
<i>c</i> (Å)	20.732(5)	12.9495(7)
α (°)	-	-
β (°)	93.994(7)	91.992(2)
γ (°)	-	-
<i>V</i> (Å ³)	7538(3)	3014.4(3)
<i>Z</i>	4	2
ρ_{calc} (Mg/m ³)	1.433	1.529
μ (Mo-K α) (mm ⁻¹)	1.459	2.131
reflections collected	22825	18283
independent reflections (<i>R</i> _{int})	6685 (0.034)	5274 (0.033)
<i>R</i> 1 [<i>I</i> > 2 σ (<i>I</i>)]	0.046	0.032
<i>wR</i> 2 (all data)	0.131	0.083

Measurement of Photocatalytic Activity.

The photocatalytic activities of the as-obtained products were monitored through photodegradation under simulated sunlight irradiation in a 50ml borosilicate glass beaker using a 400W tungsten halogen lamp as a light source. A “>400 nm” UV cut-off filter was used to completely remove any radiation below 400 nm; A “>700 nm” light cut-off filters was used to completely remove any radiation below 700 nm and to ensure illumination by near-infrared light only. The photocatalytic degradation of aqueous **RhB** (Rhodamine B) was carried out in an aqueous solution at 20 °C. In the absence of **A**, **B** or **C** as photocatalysts, no more that 5% reduction in the concentration of RhB was measured over the entire reaction time (ca. 3h), confirming that the observed reductions in RhB concentration found in studies **A**, **B** and **C** were due to photocatalysis. Photocatalytic tests were performed in duplicate for all measurements and were found to vary by no more than 5% for each data point.

0.05g of photocatalyst was added to 2×10⁻⁵mol.dm⁻³ aqueous RhB solution. Before starting the illumination, the reaction mixture was stirred for 120 min in the dark in order to reach the adsorption–

desorption equilibrium between the dye and the catalyst. At a given time interval of irradiation, 2ml aliquots were withdrawn, and then centrifuged to remove almost all the catalyst. The concentration of the remnant dye was spectrophotometrically monitored by measuring the absorbance of solutions at 550nm during the photodegradation process.

Powder Diffraction Studies of 1, 2 and 3 and A, B and C (powder XRD data for 1 have been reported in reference 8 (supporting information)).

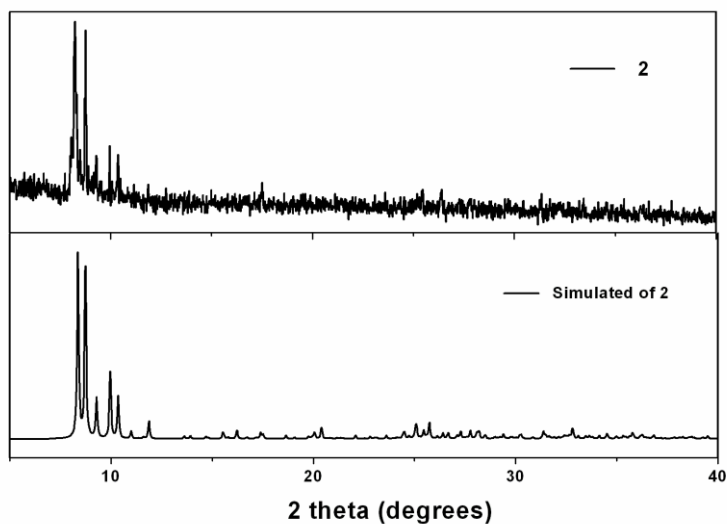


Fig. SI-1 Comparison of the powder XRD spectrum of **2** with the simulated spectrum.

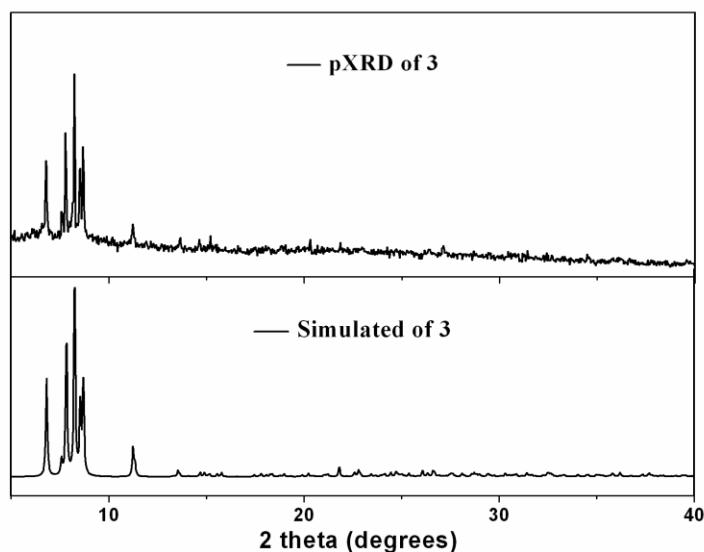


Fig. SI-2 Comparison of the powder XRD spectrum of **3** with the simulated spectrum.

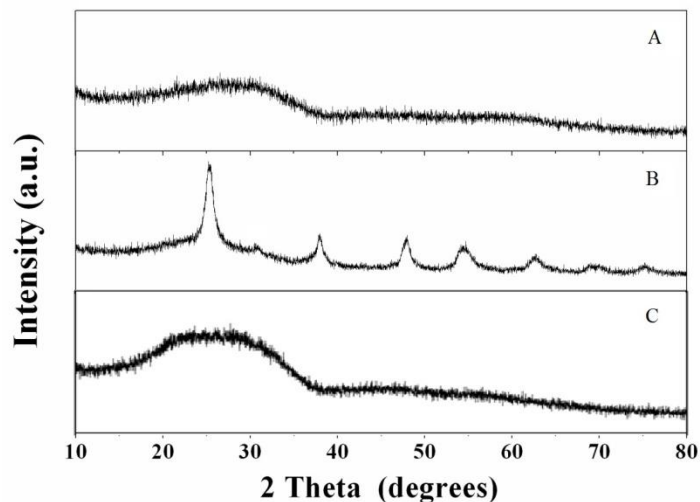


Fig. SI 3 Powder XRD on **A**, **B** and **C**. The results for sample **B** show that the TiO₂ is present in the form of anatase, whereas **A** and **C** are amorphous.

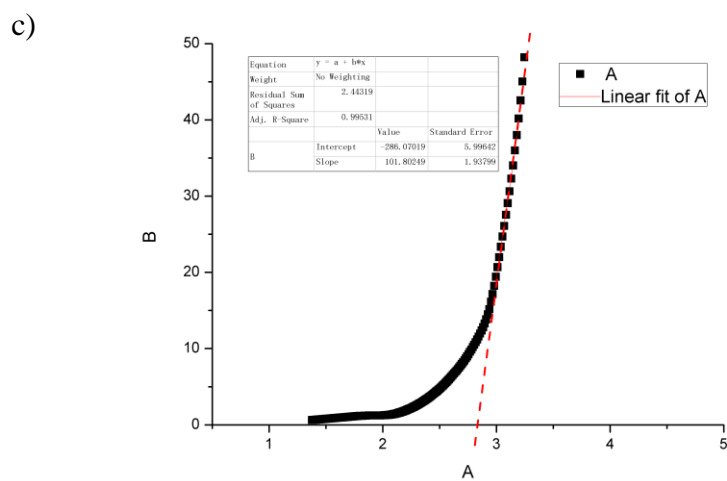
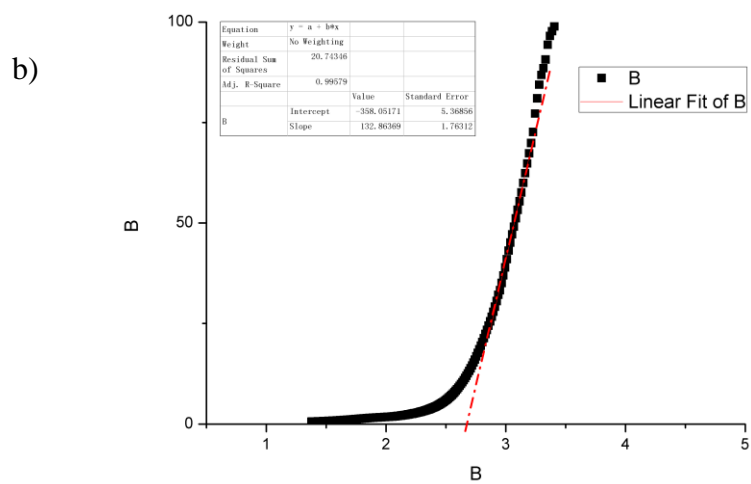
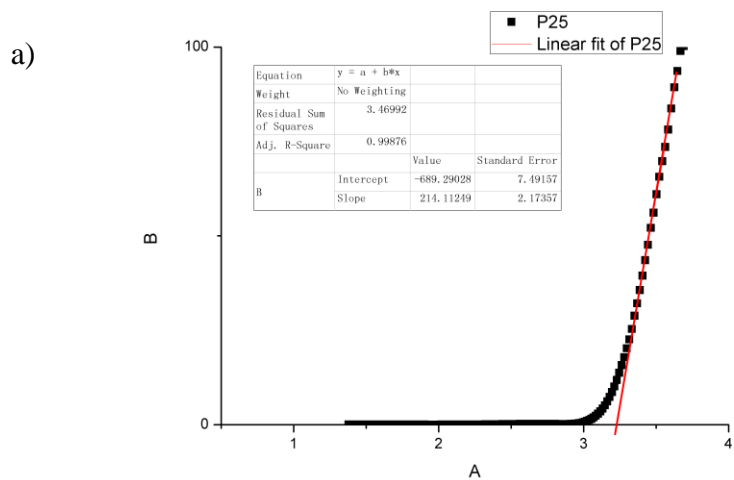
Band gap Calculations on TiO₂, A, B and C

For optical transitions near the absorption edge the absorption coefficient α (in cm⁻¹) is given by the equation,

$$\alpha = \frac{B(h\nu - E_g)^n}{h\nu} \quad \dots \text{equ. 1}$$

Where B is the absorption constant for the transition, E_g (in eV) is the bandgap, and $h\nu$ (in eV) is the photon energy. The exponent n characterizes the nature of the transition. For allowed direct and indirect transitions $n = 0.5$ and 2.0 , respectively, whereas for forbidden direct and indirect transitions $n = 1.5$ and 3.0 , respectively. (S. Adachi, *Optical Properties of Crystalline and Amorphous Semiconductors; Materials and Fundamental Properties*, Kluwer, Norwell MA, 1999, p. 280)

The UV-visible data was modeled around the absorption edge using a linear correlation (as shown below). Different values of n were explored. The best correlation was found with a value of $n = 0.5$. This also gave a sensible value for the band gap in TiO₂ (consistent with the literature value).



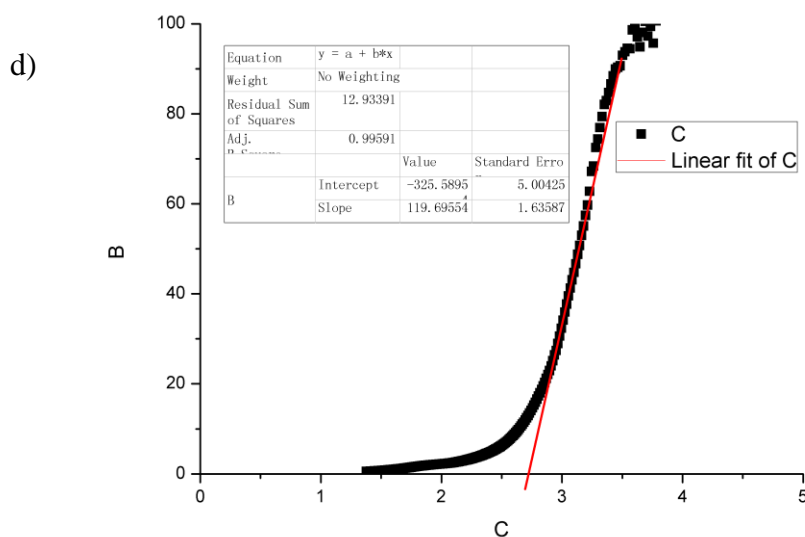


Fig. SI-4 Bandgap calculations of a) **P25** 3.20 (direct $n=0.5$); b) **A** 2.81 (direct $n=0.5$); c) **B** 2.69 (direct $n=0.5$); d) **C** 2.72 (direct $n=0.5$).

EDS Analysis (All results in atomic%)

Scanning electron microscopy images were collected using either a Jeol 5800 LV SEM with an acceleration voltage of 10 or 15keV or a Jeol T-100 SEM with an acceleration voltage of 25keV. Transmission electron microscopy images were collected using a Jeol JEM-3011 Ultra High Resolution TEM. Post image analysis was performed using the ImageJ software or INCA microanalysis package.

The surface composition of samples **A** and **B** were determined by energy dispersive spectroscopy (EDS) (Hitachi S4800). EDS data of sample **C** was collected using an Oxford Instruments Inca energy dispersive X-ray spectroscopy system attached to a Jeol 5800 LV SEM, with an acceleration voltage of 15keV or a . It was processed using the INCA microanalysis package.

Table SI-2 EDS on Sample **A** (below SEM image)

Element	Atomic Percentage
C K	7.20
O K	66.26
Ti K	25.69
Ce L	0.85

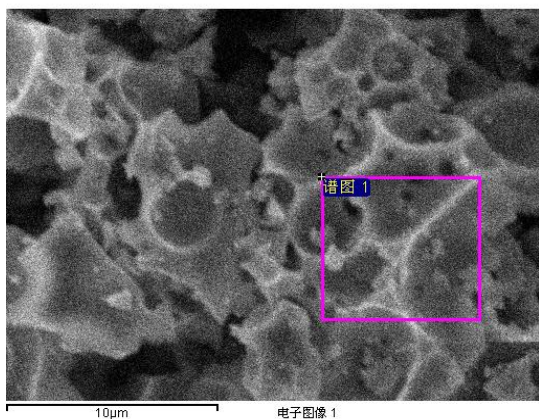


Table SI-3 EDS of Sample **B** (below SEM image)

Element	Atomic Percentage
C K	12.98
O K	62.28
Ti K	21.79
Ce L	2.95

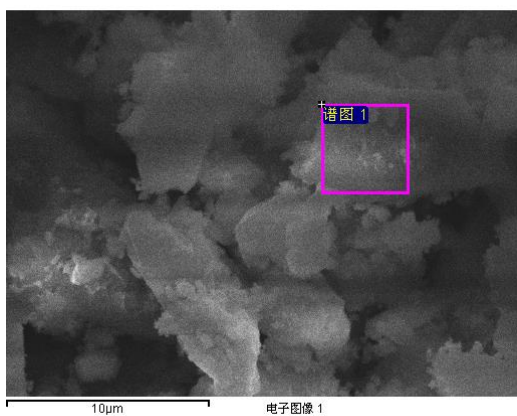
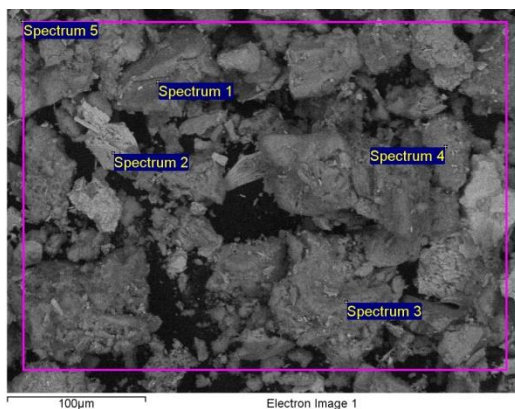


Table SI-4 EDS of Sample **C** (below SEM image)

Processing option : All elements analysed (Normalised)

Spectrum	In stats.	C	O	Ti	Ce
Spectrum 1	Yes	10.23	73.17	11.76	4.84
Spectrum 2	Yes	19.56	51.93	19.24	9.28
Spectrum 3	Yes	11.64	71.23	13.18	3.96
Spectrum 4	Yes	9.77	68.56	15.34	6.33
Spectrum 5	Yes	25.80	54.45	13.68	6.07
Mean		15.40	63.87	14.64	6.09

Std. deviation	7.04	9.92	2.87	2.02
Max.	25.80	73.17	19.24	9.28
Min.	9.77	51.93	11.76	3.96



Raman Spectroscopy

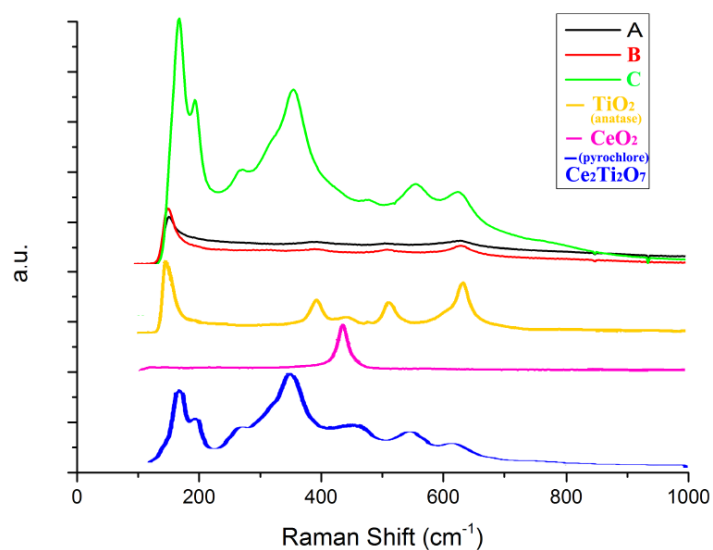


Fig. SI-5 Comparison between the Raman spectra of **A**, **B** and **C** and those of TiO_2 , CeO_2 and $\text{Ce}_2\text{Ti}_2\text{O}_7$. The Raman data for $\text{Ce}_2\text{Ti}_2\text{O}_7$ is reproduced from reference 11a.

The band at 460 cm^{-1} in the spectrum of $\text{Ce}_2\text{Ti}_2\text{O}_7$ taken from reference 11a (blue trace, Fig. SI-5) is coincident with that of CeO_2 and was attributed by the authors to CeO_2 contamination in this previous work. Significantly, this band is absent in samples of **C** and is not present in spectra of samples aged for up to 8 weeks. The Raman bands in **C** are found at 160 (lit. $165\text{ Ce}_2\text{Ti}_2\text{O}_7^{11a}$), 184 (lit. $190\text{ Ce}_2\text{Ti}_2\text{O}_7^{11a}$), 350 (lit. $350\text{ Ce}_2\text{Ti}_2\text{O}_7^{11a}$), 545 ($545\text{ Ce}_2\text{Ti}_2\text{O}_7^{11a}$), 610 ($610\text{ in TiO}_2^{11a}$) cm^{-1} and the Raman spectrum suggests that **C** is a mixture of TiO_2 and $\text{Ce}_2\text{Ti}_2\text{O}_7$ (note that the Raman absorption found in **C** at 610 cm^{-1} is also

present in an authentic sample of TiO_2 and that this TiO_2 band is also present as a contaminant in the literature Raman spectrum of $\text{Ce}_2\text{Ti}_2\text{O}_7^{11a}$). The Raman spectra of **A** and **B** illustrate both contain anatase.

Fig. SI-6 shows the effect of firing samples of **C** to up to 600°C (under N_2), resulting in an increase in crystallinity, making it easier to analyse the spectrum. There is little or no CeO_2 present in any of the samples.

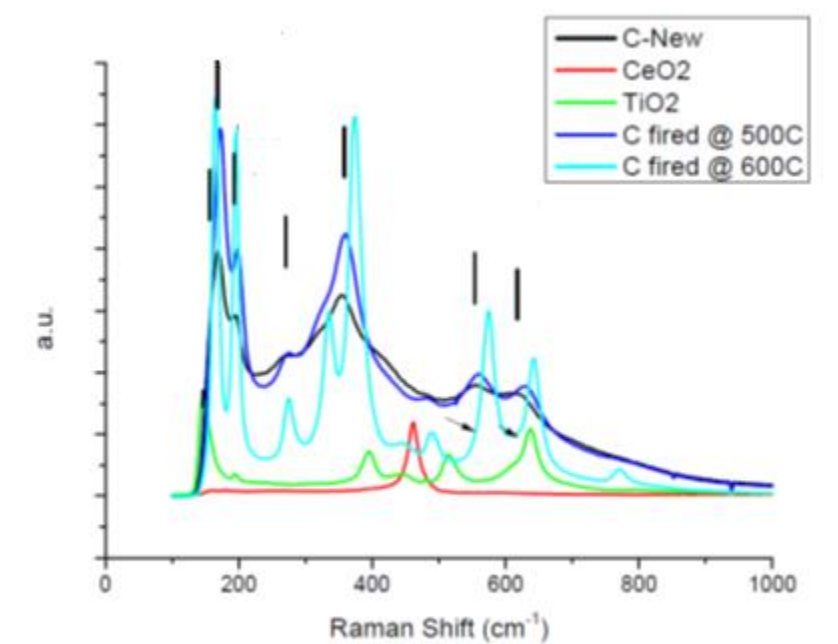


Fig. SI-6 Raman spectra showing the effects of firing sample **C**, and for comparison the Raman spectra of CeO_2 and TiO_2 .

XPS Analysis

X-ray photoelectron spectra were done on customized equipment, furnished with a High Temperature High Pressure Cell (SPECS HPC-20) with infra-red (IR) heating focused onto the sample holder. This cell, with a "chamber in chamber" design allowed the treatment of samples up to 800°C , under flow or static conditions, with pressures up to 20 bar. The cell allowed for fast transfer from the reaction chamber to the vacuum chamber, with all stages maintaining UHV conditions. Analysis was done using a non-monochromatized dual X-ray source, using Al $K\alpha$ radiation (1486.6 eV); with a hemispherical analyzer (SPECS Phoibos 100) working at fixed transmission mode and 20 eV pass energy resolution.

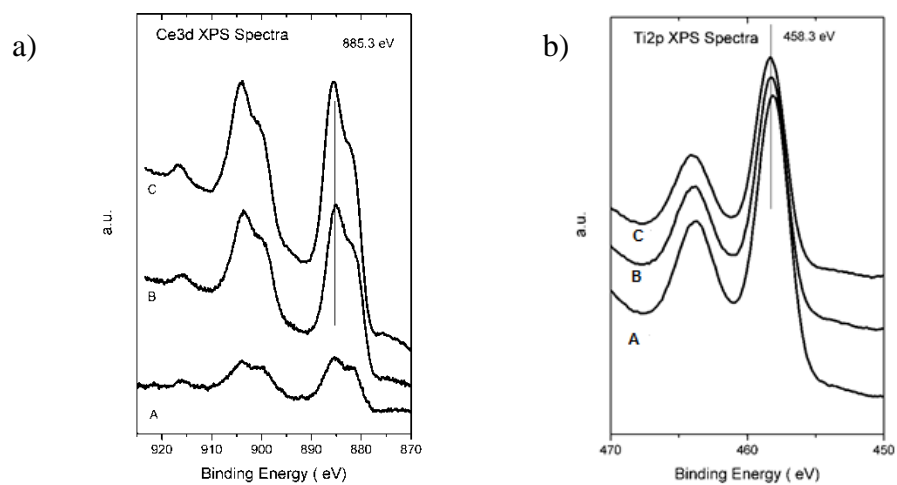


Fig. SI-7 SI- XPS signals for a) Ce 3d and b) Ti 2p regions.

Table SI-5 Quantitative results of XPS analysis of **A**, **B** and **C**.

Sample	O 1s	C 1s	Ti 2p	Ce 3d	Ti/Ce from XPS
A	53.0	26.4	19.7	0.76	26
--	--	--	--	--	--
B	49.7	29.3	18.4	2.5	7.4
--	--	--	--	--	--
C	53.6	25.6	16.7	4.0	4.1